*Biochimica et Biophysica Acta*, 506 (1978) 119—135


BBA 77884

# GALACTOSE TRANSPORT IN HUMAN ERYTHROCYTES

## THE TRANSPORT MECHANISM IS RESOLVED INTO TWO SIMPLE ASYMMETRIC ANTIPARALLEL CARRIERS

HAGAI GINSBURG
With the technical assistance of SARIT YEROUSHALM.

*Biophysics Group, Institute of Life Sciences, The Hebrew University of Jerusalem, Jerusalem (Israel)*

(Received April 29th, 1977)

## Summary

The kinetic properties of the mediated transport of galactose in human erythrocytes are investigated at 20°C. Different methodological procedures are used to acquire a complete kinetic description of the system.

Under zero-*trans* conditions the uptake of galactose is mediated by two distinctly different carriers (defined as $\alpha$ and $\beta$) having significantly different Michaelis parameters: ${}^{\alpha}K = 12.7$ mM and ${}^{\beta}K = 81.5$ mM, but similar maximal velocities, approx. 40 mM · min$^{-1}$. The zero-*trans* efflux procedure reveals apparently one single carrier with $K = 74.4$ mM and $V = 241$ mM · min$^{-1}$. Under equilibrium-exchange conditions the galactose transport is mediated apparently by a single site with $K = 146$ mM and $V = 521$ mM · min$^{-1}$.

The data for the $\alpha$-carrier are analyzed in terms of the simple carrier model as formulated by Lieb and Stein (Biochim. Biophys. Acta (1974) 373, 178). Application of several rejection criteria for the simple carrier failed to indicate lack of fitness of the $\alpha$-carrier to a simple asymmetric carrier.

From the analysis of the kinetic data it is inferred that the transport of galactose across the human erythrocyte membrane is mediated by two simple asymmetric carriers operating in antiparallel fashion. Using this model and the data of zero-*trans* and equilibrium-exchange, it is shown that the predicted half-saturation constants for both uptake and efflux in infinite-*cis* conditions fully agree with the experimentally derived values.

Further analysis of the kinetic data indicate that the translocation of the unloaded $\alpha$-carrier is the rate-limiting step in galactose uptake. Under equilibrium-exchange conditions the unloaded carrier is asymmetrically distributed across the membrane so that its concentration is 8 times higher on the inner side of the membrane. Using the value of $3.3 \cdot 10^5$ hexose carriers per cell, the turnover number of galactose exchange is $6.5 \cdot 10^4$ molecules/carrier per min.

## Introduction

The kinetic description of the hexose transport system in human red blood cells is still a subject of controversy [1—4]; the simple carrier model for this tranport system [5,6] being incompatible with the kinetic data. The several kinetic models that have been proposed (invoking diffusion barriers [7,8], various kinds of nonmobile carriers [9—11] and a two-carrier model [12]) all fail to accommodate all the kinetic data. Evidently, in order to characterize a transport system in terms of a simple carrier mechanism it is necessary to subject it to a complete analysis of kinetic data obtained by all required methodologies. For the nucleoside transport in human red blood cells [13] we have, however, recently succeeded in obtaining a complete and internally consistent kinetic description in terms of a simple asymmetric carrier as formulated by Lieb and Stein [14]. This success has encouraged us to use similar methods to re-examine the transport of galactose in red blood cells. We have confirmed the coexistence of two sites for sugar transport at the outer face of the membrane. We show that the behavior of the high-affinity site is fully compatible with a simple asymmetric carrier. We conclude that the galactose transport system is mediated by two populations of asymmetric carriers of similar kinetic properties, disposed in an antiparallel fashion in the erythrocyte membrane. A numerical simulation of an infinite-*cis* influx experiment using the kinetic parameters of the two carriers yields the Michaelis constant for this procedure which we reported previously [15].

## Experimental methods

### *Preparation of cells*

Recently outdated human blood was obtained from the blood bank. The buffy coat was removed and the cells washed four times with isotonic saline buffered with Tris · HCl, pH 7.4, at room temperature.

### *Efflux measurements*

For studies of galactose efflux, cells in a suspension at 5% hematocrit were loaded with galactose to the desired concentration by incubation at 25°C for 30 min. The loaded cells were then spun down and [$^3$H]galactose was added to give a final activity of 50 $\mu$Ci/ml of suspension. Equilibration was completed by incubation for another 10—20 min and the cells were finally packed by centrifugation.

Efflux of galactose was assayed by measuring the appearance of label in the efflux medium using the filter technique of Mawe and Hempling [16] as modified by us [13]. The loaded packed erythrocytes (approx. 50 $\mu$l) were transferred rapidly into a thermostatted beaker (20°C) containing vigorously stirred efflux medium. The tonicity of the efflux medium was adjusted to be equal to the intracellular osmolarity using NaCl in the case of zero-*trans* experiments and with galactose in the case of equilibrium-exchange experiments. At the desired time intervals samples were withdrawn through the filters and the radioactivity in aliquots of the sampled medium was counted by liquid scintillation spectrometry.

*Influx measurements*

The procedure of Ginsburg and Stein [15] was used. A 0.5 ml volume of a solution containing the desired concentration of tritium-labelled galactose in buffered saline, having a total osmolarity of 560 mosM, were added at time zero to a 50 $\mu$l volume of packed washed erythrocytes. The reaction system was vigorously mixed on a vortex mixer and at the desired time interval 8 ml of stopper solution (ice-cold buffered saline, 560 mosM, containing $1 \cdot 10^{-5}$ M $HgCl_2$, $1 \cdot 10^{-4}$ M phloretin (K and K), and 1.25 mM KI) were added under continuous vortexing. The mixture was spun down, resuspended in another 8 ml stopper solution and again centrifuged. The resulting pellet was spun through a 2 cm thick layer of ice-cold di-*n*-butyl phthalate in a polyethylene test tube. The tip containing the cells was cut off and extracted in hemolyzing solution (CsCl 4 mM/$NH_4OH$ 0.25%, v/v; Triton X-100, 50 ppm). The radioactivity of the hemolysate and its hemoglobin absorbance at 540 nm were measured. Counts trapped between the cells were determined by performing the whole procedure at 0°C and this value was subtracted from the values at the different sampling times.

*Calculations*

*Equilibrium-exchange efflux* ($^{ee}_{io}$). For equilibrium-exchange efflux we have

$$\ln \frac{C_\infty - C_t}{C_\infty} = -kt \tag{1}$$

where $C_t$ and $C_\infty$ are the counts of radioactive substrate in the efflux medium at time $t$ and at full equilibration respectively. $k$ is the corresponding rate constant which is equal to $v/S$, where $v$ is the unidirectional flux and $S$ is the substrate concentration. The slope of the natural logarithm of ln $((C_\infty - C_t)/C_\infty)$ plotted against time yields $k$. The kinetic parameters $K^{ee}$ and $V^{ee}$ in the simple Michaelis-Menten relationship: $v = V^{ee} \cdot S/(K_{ee} + S)$, are then computed either by linear least-squares regression analysis of $v/S$ against $S$ or by non-linear least-squares analysis of $v$ against $S$.

*Zero-trans efflux* ($^{zt}_{io}$). When the filter technique is used, a linear regression of net dpm against $t$ yields an intercept I at $t = 0$ which represents the initial extracellular radioactivity. A linear regression of $(\mathrm{dpm}_t - \mathrm{I})/(\mathrm{dpm}_\infty - \mathrm{I})$ against $t$ gives a slope which is equal to $v/S$. The value of $\mathrm{dpm}_\infty$ was obtained by letting the system equilibrate at 37°C for 1 h. $K^{zt}_{io}$ and $V^{zt}_{io}$ were calculated by linear regression of $v/S$ against $S$ or by non-linear least-squares analysis.

*Zero-trans influx* ($^{zt}_{oi}$). The internal concentration of galactose at each sampling time Si was calculated according to the following equation:

$$S_i = \frac{H \cdot D \cdot L}{A_i \cdot S_a} \tag{2}$$

where

$$H = \frac{A_{st} \cdot 25}{HCT_{st} \cdot 50} \tag{3}$$

$A_{st}$ is the absorbance at 540 nm of 50 $\mu$l of cell suspension at hematocrit $HCT_{st}$ which was hemolyzed in 25 ml of hemolyzing solution. $D$ is the net dpm of the sample, $A_i$ is the absorbance at 540 nm of the same sample and $S_a$ is the specific activity in dpm per galactose concentration given in mM. $L$ is a correction factor which takes into account dilutions of samples and the cellular water factor which takes into account dilutions of samples and the cellular water fraction (0.5 under the experimental conditions). The rate of uptake, $v$, is obtained directly from the slope of $S_i$ (mmol per l cell water) against time. $K_{oi}^{zt}$ and $V_{oi}^{zt}$ for the high- and low-affinity sites are obtained by non-linear least-squares analysis for the two-carrier model as described in detail by Ginsburg and Stein [15].

*Infinite cis-efflux.* The Ørskov light-scattering method as modified by Sen and Widdas [17] was used for this experiment. Cells were loaded with 300 mM galactose at 37°C and 5% hematocrit for 1 h and subsequently concentrated 10-fold. Cells were maintained at 20 ± 1°C until used in transport experiments. Into the cuvette of the Ørskov apparatus were placed 2.5-ml aliquots of 20 mM Tris buffer brought up to 610 mosM with NaCl or with NaCl + galactose at different concentrations. Into these were introduced, with a Hamilton syringe, 5 $\mu$l of the erythrocyte suspension. The change in cell volume, was recorded on a strip chart recorder. The exit times at each external galactose concentration were obtained as described by Sen and Widdas and were plotted against galactose concentration.

## Results

### *Zero-trans efflux*

For any transport system mediated by a simple carrier the ratios of the maximal transport, $V$, to the Michaelis constant, $K$, in the experimental procedures of equilibrium exchange and zero-*trans* influx and efflux must be equal. In previous publications [15,18] we reported that the $V/K$ ratio for the equilibrium exchange of galactose was equal to that of the zero-*trans* influx, but that it was significantly different from the $V/K$ ratio for the zero-*trans* efflux procedure. This discrepancy pointed to possible experimental or analylical artifacts in this system, or else to the presence of something other than a simple carrier. As an independent test we decided to re-assay the zero-*trans* efflux, this time by measuring the initial rates of galactose efflux instead of the integrated rate equation method used previously. Cells were equilibrated with various concentrations of labelled galactose as indicated in Experimental methods, and were then quickly mixed into a large volume of solution containing isotonic saline buffer to which NaCl, osmotically equivalent to the respective galactose concentration, had been added. Samples of the medium were taken using the filter technique at various time intervals and their radioactivity $dpm_t$ was determined. Fig. 1 depicts the efflux of label in mM expressed as $S_t = S\ (dpm_t - I)/(dpm_\infty - I)$ against time, from cells loaded to various concentrations of [$^3$H]galactose as indicated. The linearity of egress of galactose with time is evident and the rate was calculated from the slope. Fig. 2 shows these rates plotted against the intracellular concentration of galactose, $S$. $S$ was taken as the median cellular concentration during the sampling period since the intracellular concentration decreased considerably during that time. The line drawn

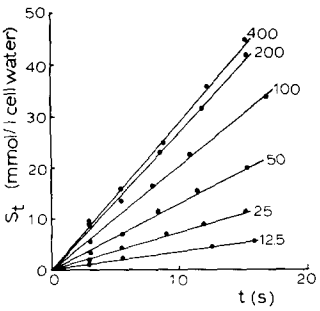


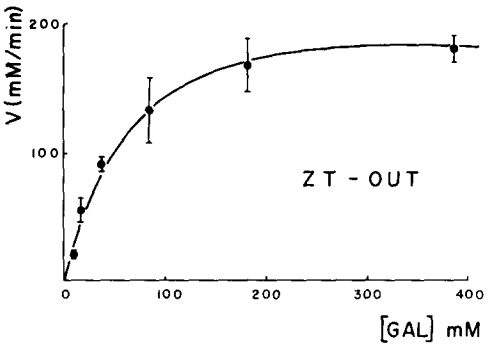


Fig. 1. Zero-*trans* efflux of galactose. The egress of galactose from cells preloaded with various concentrations of [$^3$H]galactose, is given as the depletion of intracellular galactose concentration in mM ($S_t$ = $S(\mathrm{dpm}_t - I)/(\mathrm{dpm}_\infty - I)$) as a function of time. The slope is equal to the rate of efflux. The initial intracellular concentrations of galactose are as indicated in the figure.

Fig. 2. Zero-*trans* efflux of galactose. The data of Fig. 1 are expressed as the rate of efflux against the mean intracellular concentration of galactose ([GAL]), during the sampling period. The curve was drawn using the kinetic parameters of the best fit obtained by nonlinear regression analysis: $V_{io}^{zt}$ = 208 ± 74.4 mM/min, $K_{io}^{zt}$ = 68.6 ± 27.2 mM. The vertical bars represent S.E. of quadruplicates.

is the best fit obtained from a non-linear regression analysis which uses the maximum-neighbourhood method and a simple Michaelis-Menten model. The data were also tested for the presence of an additional leak pathway or a second carrier system operating in parallel (see Ginsburg and Stein, ref. 15, for details of the analysis). Our analytical procedure failed to show any component present in a significant amount other than the single Michaelis-Menten component. The kinetic parameters derived from a series of 5 independent experiments, carried out on different days, using different blood samples, are given in Table I, together with the parameters derived in a previous study [18]. From this Table it is clear that the Michaelis constant determined by the initial-rate method is significantly different from our previously reported value while the maximal rate is not significantly different.

As a test of the validity of our experimental method we measured initial efflux rates both by the filter technique and the stopper technique simultaneously, using the same preloaded cells. A low concentration range was used 1—32 mM) to avoid large cellular volume changes. Results, as shown in Fig. 3, indicate that both techniques yield similar results. The filter technique has been chosen for subsequent work by virtue of its ease of handling and economy.

TABLE I

ZERO-*TRANS* EFFLUX OF GALACTOSE

A comparison of kinetic parameters obtained by assay of initial rates and the integrated rate equation method [18]. Both sets of data are means ± S.E. of $n$ independent experiments at 20°C.

| Method | $V$ (mM · min$^{-1}$) | $K$ (mM) | $V/K$ (min$^{-1}$) | $n$ |
|---|---|---|---|---|
| Initial rates (present work) | 241.1 ± 65.6 | 75.4 ± 24.0 | 3.20 ± 1.26 | 5 |
| Integrated rate equation [18] | 254.7 ± 96.1 | 240.6 ± 57.1 | 1.06 ± 0.04 | 4 |

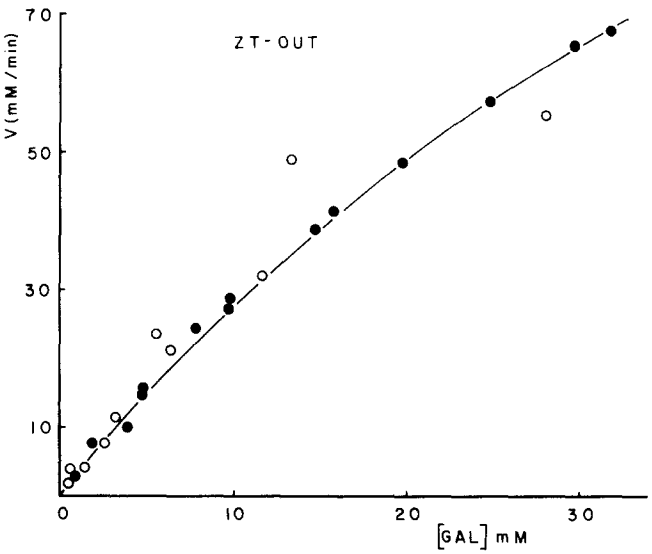


Fig. 3. Zero-*trans* efflux of galactose. Cells were preloaded with various concentrations of [$^3$H]galactose ([GAL]) (1—32 mM). Efflux was assayed by the stopping technique (○) which measures the intracellular galactose concentration, and by the filter technique (●) which measures the rate of appearance of galactose in the efflux medium.

Since the filter and the stopper techniques give indistinguishable results at least within the 1—32 mM concentration range, it is not apparently the data collection that leads to the differences listed in Table I and it is possible that errors were introduced during the analysis of the data using the integrated rate equation. Most likely to be at fault is the correction for cell volume changes that occur during galactose efflux, the correction being based on the assumption of ideal osmotic behavior. Indeed, in the method used previously [18] the cells undergo extreme volume changes during galactose egress, from isotonic to fully shrunken, which in itself could perhaps influence the rate of efflux. However, these points were not followed up any further.

*Equilibrium-exchange efflux*

The efflux of [$^3$H]galactose from cells preloaded to a desired concentration into a medium containing the same concentration of non-labeled galactose was measured by the filter technique. Usually 8—10 different substrate concentrations were used in each experiment and the rates of unidirectional efflux were obtained as indicated in Experimental methods. The linear regressions of ln $((C_\infty - C_t)/C_\infty)$ against $t$ invariably showed very high correlation coefficients. The results were subjected either to a non-linear least-squares analysis of $v$ against $S$, or to a linear least-squares fit of $S/v$ against $S$. Results of a typical experiment are shown in Fig. 4. The compilation of several experiments yielded kinetic parameters not significantly different from those reported by Ginsburg and Ram [18] as shown in Table II. The data were subjected to various analytical tests which invariably showed only one single Michaelis-Menten component

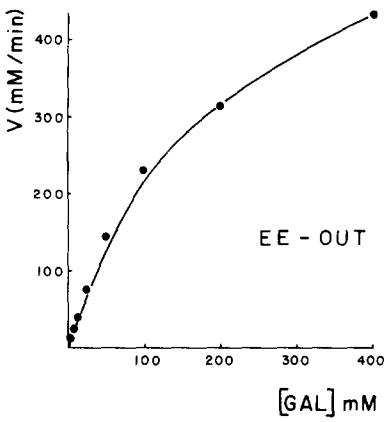


Fig. 4. Equilibrium-exchange efflux of galactose. Cells were preloaded with various concentrations of [$^3$H]galactose ([GAL]) and unidirectional efflux into media containing the same concentration of non-labeled galactose was assayed by the filter technique. Results are given as the rate of efflux as a function of galactose concentration. The curve was drawn using the parameters derived by a nonlinear least-squares regression analysis: $K^{ee}$ = 125 ± 27 mM; $V^{ee}$ = 451 ± 81 mM/min.

as in the case of the zero-*trans* efflux. The similarity between the results obtained by two independent methods serves as a test for the consistency of the experimental method.

*Zero-trans influx*

These experiments were carried out using the experimental procedure of Ginsburg and Stein [15]. Loading solutions containing different concentrations of galactose, but a constant specific activity,were used. Since the rate of mixing of the cells with medium was very fast (<1 s), the sampling time could be reduced to 2 s or less, allowing accurate estimations of initial rates even at the lowest substrate concentration used. Label trapped between the cells was determined by measuring the uptake of label by cells in the presence of cold stopping solution, or else by extrapolating the course of cellular dpm (normalized for the absorbance of the sample) against time back to $t = 0$. Both methods of correction yielded similar results. The kinetic parameters were obtained by non-linear regression analysis of $v$ against $S$ using a model with two Michaelis-Menten components in parallel, as discussed in detail before [15]. The results of these experiments revalidated our previous conclusion showing once again 2 distinct systems for the uptake of galactose into human erythrocyte. For the

TABLE II

EQUILIBRIUM-EFFLUX OF GALACTOSE

A comparison of kinetic parameters obtained by the filter technique and by the stopping technique. Both sets of data are means ± S.E. of $n$ independent experiments at 20°C.

| Method | $V$ (mM · min$^{-1}$) | $K$ (mM) | $V/K$ (min$^{-1}$) | $n$ |
|---|---|---|---|---|
| Filter (present study) | 521 ± 113 | 146 ± 5 | 3.6 ± 1.1 | 5 |
| Stopping [18] | 432 ± 4 | 138 ± 57 | 3.2 ± 0.5 | 3 |

TABLE III

ZERO-*TRANS* INFLUX OF GALACTOSE

Kinetic parameters of $\alpha$- and $\beta$-carrier as derived from non-linear least-squares analysis. Results are given as means ± S.E. of 4 independent experiments.

| Carrier | $V$ (mM/min) | $K$ (mM) | $V/K$ ($min^{-1}$) |
|---|---|---|---|
| $\alpha$ | 39.2 ± 1.7 | 12.7 ± 1.1 | 3.08 ± 0.29 |
| $\beta$ | 43.5 ± 27.8 | 81.5 ± 30.7 | 0.53 ± 0.40 |

sake of clarity we call the high-affinity transport site the $\alpha$-carrier and the low-affinity transport site the $\beta$-carrier, without alluding any mechanistic implication to the term 'carrier'. The kinetic parameters derived from several independent experiments are shown in Table III. The kinetic parameters of the $\alpha$-carrier are very similar to those reported by us previously, while those of the $\beta$-carrier are different, but not significantly so. Usually the values for the $\alpha$-carrier are very reproducible while those of the $\beta$-carrier vary considerably from one blood sample to the other. This is probably due to the fact that the highest galactose concentration used was 500 mM which may be too low for an accurate determination of a system having a Michaelis constant of about 100 mM.

*Infinite-cis efflux*

The Ørskov method, as modified by Sen and Widdas [17], is a widely used and well characterized procedure for measurements of net sugar efflux from erythrocytes. It was chosen here for its relative simplicity and economy. Fig. 5 shows the 'exit' times, computed as detailed in [17], from cells preloaded to 300 mM galactose into media containing various concentrations of galactose, in a typical experiment. The intercept on the abcissa yields directly the Michaelis constant for infinite-*cis* efflux. The mean value (± S.E.; $n$ = 4) for $K_{io}^{ic}$ was 19.2 ± 1.5 mM.

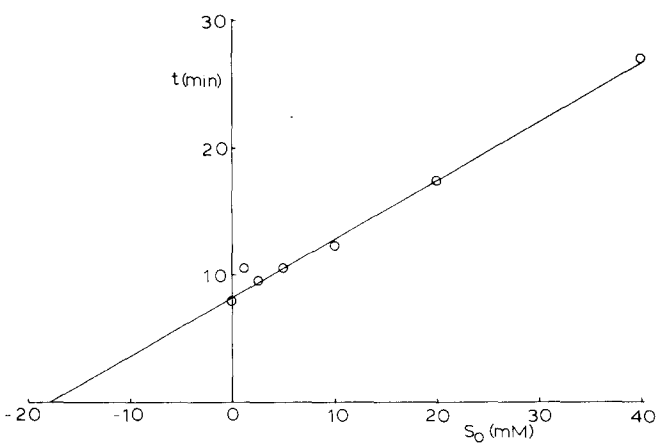


Fig. 5. Infinite-*cis* efflux of galactose from cells preloaded to 300 mM. The exit times (in min) are plotted versus the extracellular galactose concentration. The line was drawn by least-squares linear regression, yielding $K_{io}^{ic}$ = 18.3 mM with a correlation coefficient of 0.982.

## Discussion

In this discussion we will test the following proposition: the galactose transport system of human erythrocytes displays a kinetic behavior which is compatible with two asymmetric carriers operating in an anti-parallel fashion.

We have already shown conclusively [15] and we now confirm in the present work (Table III) that the zero-*trans* uptake of galactose is mediated by two carriers having different affinities for the sugar, but similar maximal rates of uptake. From Table IV it can be readily seen that the $V/K$ ratios for the total equilibrium-exchange and zero-*trans* efflux are identical with the $V/K$ ratio for zero-*trans* influx using the $\alpha$-carrier, within experimental error. Since the identity of the $V/K$ ratios obtained by various experimental procedures is a necessary condition for the applicability of the simple carrier, the $\alpha$-carrier, at least, may be a simple carrier. The $\alpha$-carrier (Tables III and IV) mediates a major part of the transport of galactose across the membrane of the human erythrocyte.

Before we proceed to analyze further the $\alpha$-carrier, it is necessary to attempt an evaluation of the contribution of the $\beta$-carrier to efflux under both zero-*trans* and equilibrium-exchange conditions. Now for the $\alpha$-carrier the maximal zero-*trans* influx is approx. 1/6 of the efflux. Were the same ratio to hold also for the $\beta$-carrier, but in the reverse direction, then the contribution of the $\beta$-carrier to zero-*trans* efflux would be 1/6 of the relevant maximal influx, giving 8 mM $\cdot$ min$^{-1}$. This is 1/30 of the measured total zero-*trans* efflux and could not be detected by our experimental procedure. It is also possible to argue that the $K_m$ for equilibrium exchange for the $\beta$-carrier might be close enough to the $K_m$ for the $\alpha$-carrier so that the two separate sites could not be identified by the equilibrium-exchange procedure.

Suppose that the maximal rate of exchange mediated by the $\beta$-carrier is twice the maximal zero-*trans* influx (by analogy with the $\alpha$-carrier), hence some 87 mM $\cdot$ min$^{-1}$. Then from the relevant $V/K$ ratio of 0.53 (Table III) we obtain ${}^{\beta}K^{ee}$ = 164 mM which is not sufficiently different from $K^{ee}$ = 146 mM, derived directly from the data of equilibrium-exchange total efflux (Table II). On this basis, further analysis of the $\alpha$-carrier will use the value of $V^{ee}$ = 434 mM $\cdot$ min$^{-1}$ (= 521 — 87) as the maximal equilibrium-exchange efflux. It is true to say, however, that unless the $\alpha$-carrier can be inactivated independently from the $\beta$-carrier or vice versa, a full kinetic description of the $\beta$-carrier is impossible and that of the $\alpha$-carrier must remain tentative.

We proceed, on this kinetic basis, to analyze the data of the $\alpha$-carrier, accord-

TABLE IV

COMPILATION OF KINETIC DATA FOR ZERO-*TRANS* AND EQUILIBRIUM-EXCHANGE EFFLUX (io) AND THE $\alpha$-CARRIER (HIGH-AFFINITY COMPONENT) OF THE ZERO-*TRANS* INFLUX (oi) AT 20°C

Data are presented as weighted means and S.E. of $n$ experiments in each procedure.

| Procedure | $V$ (mM/min) | $K$ (mM) | $V/K$ (min$^{-1}$) | $n$ |
|---|---|---|---|---|
| ee-io | 434.0 ± 112.8 | 145.8 ± 31.6 | 2.98 ± 1.09 | 4 |
| zt-io | 241.1 ± 65.5 | 74.4 ± 23.9 | 3.24 ± 1.36 | 4 |
| zt($\alpha$)oi | 39.2 ± 1.7 | 12.7 ± 1.1 | 3.08 ± 0.29 | 5 |

ing to the formalism of the one-complex model of a simple carrier as given by Lieb and Stein [14].

For a simple carrier the unidirectional flux from inside to outside is given by

$$v_{io} = \frac{KS_i + S_iS_o}{K^2R_{oo} + KR_{io}S_i + KR_{oi}S_o + R_{ee}S_iS_o} \tag{4}$$

where $K$ is a basic measurable transport parameter related to the half-saturation concentrations, $S_i$ and $S_o$ are the respective intracellular and extracellular substrate concentrations. The $R$ symbols represent basic measurable parameters related to the maximal rates of transport:

$$R_{io} = 1/V_{io}^{zt}; \quad R_{oi} = 1/V_{oi}^{zt}; \quad R_{ee} = 1/V^{ee} \tag{5}$$

and also

$$R_{io} + R_{oi} = R_{ee} + R_{oo} \tag{6}$$

where $R_{oo}$ is the resistance to movement experienced by the unloaded carrier. The experimental parameters in terms of $R$ values and $K$ are given in the Appendix (Table AI). We derive $R_{oo}$ from Eqns. 5 and 6 using the maximal velocities given in Table IV. Thus:

$$R_{oo} = R_{io} + R_{oi} - R_{ee} = 0.0041 + 0.0255 - 0.0023 = 0.0273 \text{ min} \cdot \text{mM}^{-1}$$

The standard error of $R_{oo}$ is equal to $5 \cdot 10^{-4}$ min $\cdot$ mM$^{-1}$.

We first use the rejection criteria introduced by Hankin, Lieb and Stein [19] in conjunction with the transport of glucose in erythrocytes. Their first criterion is based on the relation

$$Q + 1 = \frac{K^{ee} \cdot R_{oo} \cdot R_{ee}}{K_{io}^{zt} \cdot R_{io}^2} + \frac{K_{io}^{zt}}{K^{ee}} \tag{7}$$

which can be obtained readily from Table AI in the Appendix and where $Q$, the asymmetry factor, is given by

$$Q = \frac{K_{io}^{zt}}{K_{oi}^{zt}} = \frac{V_{io}^{zt}}{V_{oi}^{zt}} \tag{8}$$

From Table IV we find: $K_{io}^{zt}/K_{oi}^{zt} = 5.85 \pm 1.9$ and $V_{io}^{zt}/V_{oi}^{zt} = 6.15 \pm 1.7$, so $Q = 6.0 \pm 1.8$. Since the right-hand side of Eqn. 7 gives $7.75 \pm 1.2$ and $Q + 1 = 7.0 \pm 1.8$, the simple carrier cannot be rejected. The second rejection criterion is also based on Eqn. 7 but is transformed into a quadratic expression in $K^{ee}$:

$$\frac{(K^{ee})^2 \cdot R_{oo} \cdot R_{ee}}{K_{io}^{zt} \cdot R_{io}^2} - (Q + 1) \cdot K^{ee} + K_{io}^{zt} = 0 \tag{9}$$

which yields

$$Q + 1 \geqslant 2(R_{oo}R_{ee})^{1/2} R_{io}^{-1} \tag{10}$$

The right-hand side of Eqn. 10 is equal to $3.9 \pm 1.6$, i.e., smaller than $Q + 1$. Here also the simple carrier is not rejected.

The kinetic parameters derived from the equilibrium-exchange and the zero-*trans* procedures are in effect sufficient to fully describe a simple carrier mechanism and for the application of rejection criteria. However, to test the internal consistency of the kinetic analysis, another experimental procedure, the infinite-*cis* procedure, can also be applied. This procedure consists of measuring net fluxes by setting the *cis* side at high concentration of substrate relative to $K$ while the concentration at the *trans* side is varied. $K^{ic}$ is defined as that *trans* concentration which reduces the maximal net flux by one-half. We measured previously the infinite-*cis* uptake of galactose [15] and we anticipated then the detection of both a high- and a low-affinity site on the inner face of the membrane if indeed two asymmetric carriers were operating in parallel. We found only one site with $K^{ic}$ of approx. 21—25 mM. We shall now attempt to interpret this finding based on our present model of two antiparallel carriers.

The net infinite-*cis* influx contributed by the two types of carrier is given by:

$$NET_{oi}^{ic} = \frac{K^{\alpha}}{K^{\alpha}R_{oi}^{\alpha} + R_{ee}^{\alpha}S_i} + \frac{K^{\beta}}{K^{\beta}R_{oi}^{\beta} + R_{ee}^{\beta}S_i} \tag{11}$$

And for each carrier

$$K = \frac{K_{oi}^{zt}}{V_{oi}^{zt}(R_{io} - R_{ee})} = \frac{K_{oi}^{zt}}{1 + Q - V_{oi}^{zt}/V_{ee}} \tag{12}$$

Having a tentative kinetic description of the $\alpha$-carrier, knowing that ${}^{\beta}V_{oi}^{zt}$ = 43.5 mM · min$^{-1}$ and ${}^{\beta}K_{oi}^{zt}$ = 81.5 mM and setting ${}^{\beta}V^{ee} = {}^{\beta}V_{oi}^{zt} \cdot 2$ = 87 mM · min$^{-1}$, we might simulate an infinite-*cis* uptake experiment by setting these values into Eqn. 11 with different values of ${}^{\beta}Q$, the asymmetry factor for the $\beta$-carrier. The result of such simulation is shown in Fig. 6. We can see from this figure that the internal substrate concentration at which the total maximal rate of sugar uptake (82.6 mM · min$^{-1}$) is reduced to one-half coincides precisely

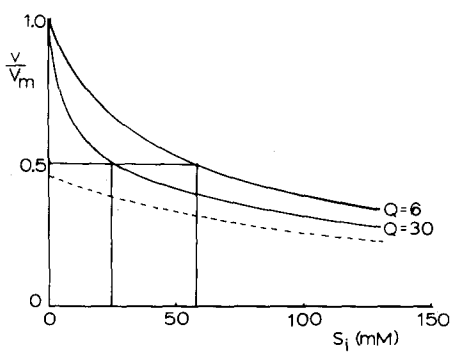


**Fig. 6. Simulation of net galactose influx as a function of intracellular galactose concentration. Eqn. 10 was used with the following kinetic parameters: For the $\alpha$-carrier: $K$ = 11.1 mM; $R_{oi}$ = 2.55 · 10$^{-2}$ min/mM; $R_{ee}$ = 1.92 · 10$^{-3}$ min/mM. For the $\beta$-carrier $K$ was calculated from Eqn. 11 with $K_{oi}^{zt}$ = 81.5 mM; $V_{oi}^{zt}/V_{ee}$ = 2; and different values of $Q$ as indicated. $R_{oi}$ = 2.3 · 10$^{-2}$ min/mM and $R_{ee}$ was set at one half of that value. The dashed line indicates the contribution of the $\alpha$-carrier. The horizontal line indicates 50% of the maximal velocity and the left vertical line shows the values of $K_{oi}^{ic}$ obtained experimentally [16].**

with the experimentally derived $K_{oi}^{ic}$ of 21—25 mM. This fitting is obtained with an asymmetry factor $Q = 30$. When $Q = 6$ was used in the simulation, the resulting $K_{oi}^{ic}$ was about 60 mM, significantly different from the experimental value. Thus, the asymmetry of the β-carrier appears to be much larger than that of the α-carrier. From a comparison of the continuous curves in Fig. 6 (which represent the net flux mediated by both carriers) and the dashed line which depicts the contribution of the α-carrier alone, it can be seen that at $S_i \approx 50$ mM the α-carrier is the sole contributor to net uptake. The value of $K_{oi}^{ic}$ for the α-carrier is equal to that internal substrate concentration where $NET_{oi}^{ic} = {}^{\alpha}V_{oi}^{zt}/2 = 19.6$ mM · min$^{-1}$, i.e., ${}^{\alpha}K_{oi}^{ic} = 147$ mM. ${}^{\alpha}K_{oi}^{ic}$ can also be computed from the following relation [14]:

$$K_{oi}^{ic} = \frac{K_{oi}^{zt} \cdot R_{oi}^2}{R_{oo} \cdot R_{ee}} \tag{13}$$

which, upon using the kinetic parameters of the α-carrier (Table IV), yields 131 mM, not significantly different from 147 mM. It can be concluded that the two values are in accord with each other and internally consistent with the kinetic properties which characterize a simple carrier mechanism. The net infinite-*cis* efflux can also be described by Eqn. 11 after interchanging the indices i and o. It can be seen readily that although the β-carrier will be stopped only at relatively high external concentrations of galactose ($R_{ee}^{\beta} << R_{io}^{\beta}$), its contribution is relatively small and most of the efflux is carried out by the α-carrier. Thus $K_{io}^{ic}$ can be derived within a good approximation from the kinetic parameters of the α-carrier using the reverse of Eqn. 13. Thus,

$$K_{io}^{ic} = \frac{K_{io}^{zt} \cdot R_{io}^2}{R_{oo} \cdot R_{ee}} = 20.2 \text{ mM}$$

The computed constant is practically equal to the experimental value of 19.2 ± 1.5 mM. This equality displays the internal consistency of the α-carrier as a simple asymmetric carrier. However, results obtained by this procedure cannot lend further support for the existence of the β-carrier.

We would like then to conclude that the mechanism of the mediated transport of galactose across the human erythrocyte membrane is compatible with two asymmetric carriers operating in an antiparallel fashion. It is very possible that both types of carriers are essentially identical except for their opposite polarity with respect to the membrane. This is concluded from the similarities of ${}^{\alpha}K_{io}^{zt}$ and ${}^{\beta}K_{oi}^{zt}$ (approx. 80 mM) and of the intrinsic parameter $K$: 11.1 mM for the α-carrier and about 15 mM for the β-carrier. If such identity does exist then it is possible to estimate the relative amount, $n$, of carriers of each type by a relation derived by Eilam (ref. 12, equation 14) $n = {}^{\alpha}V_{io}^{zt}/{}^{\beta}V_{oi}^{zt} = 5.54$, i.e., 15% of the total number of carriers are oriented such that their low-affinity site is facing the extracellular space. This is an upper limit estimate since the asymmetry of the β-carrier is certainly much higher than that of the α-carrier.

We are entitled to calculate further the kinetic parameters of the α-carrier in terms of a simple carrier. There are four independent measurable parameters, i.e., one Michaelis constant (either $K_{io}^{zt}$, $K_{oi}^{zt}$ or $K^{ee}$), $V_{io}^{zt}$, $V_{oi}^{zt}$ and $V^{ee}$ but five independent molecular rate constants, resulting from the following constraint

(see Fig. AI):

$$f_2 b_1 k_1 = f_1 b_2 k_2 \tag{14}$$

Lieb and Stein [14] showed that although the exact values of all possible ratios of rate constants cannot be computed for the simple carrier, the bounds for some ratios can be obtained. When the ratios of the $R$ parameters are expressed in terms of molecular rate constants (see Appendix), the upper and lower bounds for $k_1/k_2$ are given by:

$$\frac{R_{oo} - R_{oi}}{R_{oi}} < \frac{k_1}{k_2} < \frac{R_{io}}{R_{oo} - R_{io}} \tag{15}$$

which, in the case of the $\alpha$-carrier, is

$$0.071 < \frac{k_1}{k_2} < 0.177$$

The lower bounds for $b_1/k_1$ and $b_2/k_2$ are found in the same way:

$$\frac{b_1}{k_1} > \frac{R_{oi} - R_{ee}}{R_{ee}} = 10.1 \text{ and } \frac{b_2}{k_2} > \frac{R_{io} - R_{ee}}{R_{ee}} = 0.78$$

Taking the median value of $k_1/k_2$ we can calculate readily other ratios of rate constants. Thus, the ratio of the dissociation rate constants is $b_1/b_2 = 1.6$ and that of the association rate constants is $f_1/f_2 = 0.2$.

There are several important implications to these inequalities and the derived ratios. First, the asymmetry of the $\alpha$-carrier stems primarily from the fact that in the zero-*trans* influx conditions the movement of the unloaded carrier is rate-limiting since $b_1 = 10.1\ k_1$. This is also true in the case of the uridine carrier [13]. However, in the zero-*trans* efflux conditions the dissociation rate constant is similar to the translocation rate constant of the unloaded carrier $k_2$ inasmuch as $b_2 = 0.78\ k_2$. Wilbrandt [20] has also suggested that the translocation of the complex is not necessarily the rate-limiting step in the transport of hexoses across the erythrocyte membrane. Second, although $b_1/b_2 = 1.6$, as calculated with the median value of $k_1/k_2$, if one uses the lower bound of $k_1/k_2$ one gets $b_1/b_2 = 0.92$. This result implies that the structural asymmetry of the erythrocyte membrane with respect to proteins [21] and lipids [22] may not affect the rate of dissociation of the complex. The opposite is true for the association rate constants. When the median value of $k_1/k_2$ and the resulting $b_1/b_2 = 1.6$ are used, $f_1/f_2 = 0.2$, but if the lower bound of $k_1/k_2$ is used, then $f_1/f_2 = 0.065$. This is undoubtedly another source for the asymmetry of the carrier mechanism, although the structural and the molecular basis for it must await further investigation. Third, the different ratios of molecular rate constants can be used to compute the relative distribution of free carriers on both sides of the membrane. Stein and Lieb [23] have shown that at steady state the concentration of the free carrier at the inner side of the membrane is given by

$$E_1 = \frac{T(b_1 k_2 + b_2 k_2 + b_1 f_2 S_2)}{\Sigma} \tag{16}$$

$$E_2 = \frac{T(b_2 k_1 + b_1 k_1 + b_2 f_1 S_1)}{\Sigma} \tag{17}$$

where $T$ is the total carrier concentration, $f_1$, $f_2$, $b_1$, $b_2$, $k_1$ and $k_2$ are defined in Fig. AI.

$$\Sigma = (b_1 + b_2)(k_1 + k_2) + (b_2 + k_2)f_1S_1 + (b_1 + k_1)f_2S_2 + f_1f_2S_1S_2 \tag{18}$$

From the principle of microscopic reversibility which states that

$$b_1k_1f_2 = b_2k_2f_1 \tag{19}$$

and from the fact that under equilibrium conditions

$$S_1 = S_2 = S \tag{20}$$

we arrive at the following equality for the ratio of carrier concentration:

$$\frac{E_1}{E_2} = \frac{b_1k_2 + b_2k_2 + b_1f_2S}{b_2k_1 + b_1k_1 + b_2f_1S} = \frac{k_2}{k_1} \tag{21}$$

In addition $f/b$ is the association constant of the carrier · substrate complex on either side of the membrane, hence

$$f_1/b_1 = ES_1/E \cdot S_1 \text{ and } f_2/b_2 = ES_2/E \cdot S_2 \tag{22}$$

Combining Eqns. 20, 21 and 22 we obtain

$$\frac{b_1k_1f_2}{b_2k_2f_1} = \frac{ES_2}{ES_1} \tag{23}$$

and finally, using Eqns. 19 and 23 we arrive at $ES_1 = ES_2$. This indicates that under equilibrium-exchange conditions, the concentration of carrier · substrate complex (i.e., loaded carrier) is equal at both sides of the membrane. Thus, any observed asymmetry should stem from uneven distributions of free carrier. Thus, $E_1/E_2 = k_2/k_1 = 8$, which means that the concentration of free carrier on the inner side of the membrane is 8 times higher than that on the outer side. It should be emphasized however, that the present treatment does not allow distinction between distribution of carriers as compared to conformational states of carriers. If we use the value of $1.43 \cdot 10^{13}$ cells per l cell water and each cell has $3.3 \cdot 10^5$ hexose binding sites [24] of which at least 85% are $\alpha$-carriers, then the calculated turnover rate under equilibrium-exchange conditions ($V^{ee} = 432$ mM · min$^{-1}$) is approx. $6.5 \cdot 10^4$ molecules/carrier per min at 20°C.

Such turnover number probably excludes the possibility that the hexose carrier in human erythrocytes is a simple mobile carrier and suggests some kind of a gating mechanism which is kinetically indistinguishable from mobile carrier-mediated transport kinetics.

The present suggested mechanism for sugar transport in human erythrocytes is based on experimental evidence obtained by the zero-*trans*, equilibrium-exchange and the infinite-*cis* procedures. It is possible that specifically devised experiments of countertransport (hetero-exchange) could be used to further examine the two antiparallel asymmetric carriers model.

## Appendix

The results of the present work are analyzed according to Lieb and Stein [14]. There the one-complex form of the simple carrier is treated and the

steady-state solutions are given. Only relations relevant to the present work are brought into this Appendix.

The unidirectional flux of a permeant from inside to the outside of the cell is given by:

$$v_{io} = \frac{KS_i + S_iS_o}{K^2R_{oo} + KR_{io}S_i + KR_{oi}S_o + R_{ee}S_iS_o} \tag{A1}$$

The unidirectional flux in the opposite direction is obtained by interchanging symbols i and o. $K$ is an intrinsic parameter related to the half saturation constant, $R$ symbols are defined in Table AI and $S_i$ and $S_o$ are the internal and external permeant concentrations respectively.

In the zero-*trans* efflux procedure, $S_o = 0$ and Eqn. AI reduces to

$$v_{io}^{zt} = \frac{S_i}{KR_{oo} + R_{io}S_i} \tag{A2}$$

Interchanging symbols i and o yields the corresponding relation for zero-*trans* uptake.

In the equilibrium-exchange procedure when $S_i = S_o$, Eqn. AI reduces to

$$v_{io}^{ee} = v_{oi}^{ee} = \frac{S_i}{R_{oo}K + R_{ee}S_i} = \frac{S_o}{R_{oo}K + R_{ee}S_o} \tag{A3}$$

This is based on the relation $R_{ee} + R_{oo} = R_{io} + R_{oi}$.

In the infinite-*cis* procedure, when $S_i$ is limitingly large, Eqn. AI reduces to

$$NET_{io}^{ic} = \frac{K}{KR_{io} + R_{ee}S_o} \tag{A4}$$

The corresponding result for the procedure in the other direction is obtained

TABLE AI

INTERPRETATION OF EXPERIMENTAL DATA IN TERMS OF BASIC PARAMETERS

| Experimental procedure | Maximal velocity | Michaelis constant |
|---|---|---|
| Zero-*trans* Efflux | $V_{io}^{zt} = \frac{1}{R_{io}}$ | $K_{io}^{zt} = K\frac{R_{oo}}{R_{io}}$ |
| Influx | $V_{oi}^{zt} = \frac{1}{R_{oi}}$ | $K_{oi}^{zt} = K\frac{R_{oo}}{R_{oi}}$ |
| Infinite-*cis* Efflux | $V_{io}^{ic} = \frac{1}{R_{io}}$ | $K_{io}^{ic} = K\frac{R_{io}}{R_{ee}} = \frac{K_{io}^{zt} \cdot R_{io}^2}{R_{oo} \cdot R_{ee}}$ |
| Influx | $V_{oi}^{ic} = \frac{1}{R_{oi}}$ | $K_{oi}^{ic} = K\frac{R_{oi}}{R_{ee}} = \frac{K_{oi}^{zt} \cdot R_{oi}^2}{R_{oo} \cdot R_{ee}}$ |
| Equilibrium exchange | $V_{io}^{ee} = V_{oi}^{ee} = \frac{1}{R_{ee}}$ | $K^{ee} = K\frac{R_{oo}}{R_{ee}}$ |

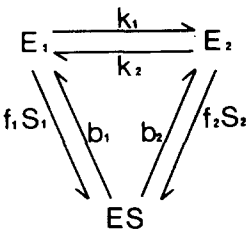


Fig. AI. The one-complex form of the simple carrier.

by interchanging i and o. The maximal velocity is the same as in the zero-*trans* procedure while $K^{ic}$ is that trans concentration at which the maximal velocity is reduced to one half.

From the above equations the experimental data are interpreted in terms of basic measurable parameters in Table AI.

The basic parameters can be expressed in terms of the molecular rate constants $k$, $f$ and $b$ (see text and Fig. AI) as shown in Table AII.

From this table it can be seen that there are four independent measurable parameters and five independent molecular rate constants. Therefore, the rate constants cannot be computed exactly but certain bounds for the ratios of molecular constants can be obtained. Bounds derived from Eqns. 25 and 26 and Table III of Lieb and Stein [14] are given in Table AIII.

TABLE AII

DEFINITION OF BASIC MOLECULAR PARAMETERS IN TERMS OF RATE CONSTANTS

$$nR_{io} = \frac{1}{b_2} + \frac{1}{k_2} \qquad K = \frac{b_1 k_1}{f_1}\left(\frac{1}{b_1} + \frac{1}{b_2}\right)$$

$$nR_{oi} = \frac{1}{b_1} + \frac{1}{k_2} \qquad \text{Constraint: } f_2 b_1 k_1 = f_1 b_2 k_2$$

$$nR_{oo} = \frac{1}{k_1} + \frac{1}{k_2}$$

$n$ is the total number of carriers per unit area of membrane while $nR$ is the specific resistance of the membrane to the particular carrier-form.

$$nR_{ee} = \frac{1}{b_1} + \frac{1}{b_2}$$

TABLE AIII

UPPER AND LOWER BOUNDS FOR RATIOS OF RATE CONSTANTS IN TERMS OF BASIC MEASURABLE PARAMETERS

$$\frac{R_{ee} - R_{oi}}{R_{oi}} < \frac{b_1}{b_2} < \frac{R_{io}}{R_{ee} - R_{io}} \qquad \frac{R_{oi} - R_{ee}}{R_{ee}} < \frac{b_1}{k_1} < \frac{R_{oo}}{R_{oi} - R_{oo}}$$

$$\frac{R_{oo} - R_{oi}}{R_{oi}} < \frac{k_1}{k_2} < \frac{R_{io}}{R_{oo} - R_{io}} \qquad \frac{R_{io} - R_{ee}}{R_{ee}} < \frac{b_2}{k_2} < \frac{R_{oo}}{R_{io} - R_{oo}}$$

## Acknowledgements

I am very grateful to Prof. W.D. Stein for his encouragement and criticism and to the Professor Philip Stein Fellowship Fund generously sponsored by the Sagov Industrial Management Co. Ltd. of South Africa, for financial support.

## References

1 Lieb, W.R. and Stein, W.E. (1972) Biochim. Biophys. Acta 269, 187—207
2 LeFevre, P.G. (1975a) in Current Topics in Membranes and Transport, (Bronner, F. and Kleinzeller, A., eds.), Vol. 7, pp. 109—215, Academic Press, New York
3 LeFevre, P.G. (1975b) Ann. N.Y. Acad. Sci. 264, 398—413
4 Jung, C.Y. (1975) in The Red Blood Cell (Surgenor, D. MacN., ed.), 2nd edn., Chap. 16, pp. 705—751, Academic Press, New York
5 LeFevre, P.G. (1954) Symp. Soc. Exp. Biol. 8, 118—135
6 Widdas, W.F. (1954) J. Physiol. (London) 125, 163
7 Regen, D.M. and Tarpley, H.L. (1974) Biochim. Biophys. Acta 332, 218—233
8 Batt, E.R. and Schachter, D. (1973) J. Clin. Invest. 52, 1686—1697
9 Naftalin, R.J. (1970) Biochim. Biophys. J. 10, 585—609
11 LeFevre, P.G. (1973) J. Membrane Biol. 11, 1—19
12 Eilam, Y. (1975) Biochim. Biophys. Acta 401, 349—363
13 Cabantchik, Z.I. and Ginsburg, H. (1977) J. Gen. Physiol. 69, 75—96
14 Lieb, W.R. and Stein, W.D. (1974) Biochim. Biophys. Acta 373, 178—196
15 Ginsburg, H. and Stein, W.D. (1975) Biochim. Biophys. Acta 382, 353—368
16 Mawe, R.C. and Hempling, H.G. (1965) J. Cell Comp. Physiol. 66, 95—104
17 Sen, A.K. and Widdas, W.F. (1962) J. Physiol. (London) 160, 392—403
18 Ginsburg, H. and Ram. D. (1975) Biochim. Biophys. Acta 382, 369—376
19 Hankin, B.L., Lieb, W.R. and Stein, W.D. (1972) Biochim. Biophys. Acta 288, 151—166
20 Wilbrandt, W. (1972) in Passive Permeability of Cell Membranes (Kreuzer, F. and Slegers, J.F., eds.), Vol. 3, pp. 79—99, Plenum Press, New York
21 Steck, T.L. (1974) J. Cell. Biol. 62, 1—19
22 Zwaal, R.F.A., Roelofsen, B. and Colley, C.M. (1973) Biochim. Biophys. Acta 300, 159—182
23 Stein, W.D. and Lieb, W.R. (1973) Israel J. Chem. 11, 325—339
24 Taverna, R.D. and Langdon, R.G. (1973) Biochim. Biophys. Acta 323, 207—219